# A51E-0116: Actinic flux measurements and photolysis frequencies enhancements near clouds during DC3 and TORERO


**S. R. Hall[1], K. Ullmann[1], K.S. Schmidt[2], B. Kindel[2], J.W. Hair[3]**

*1. National Center for Atmospheric Research (NCAR), Boulder, CO 2. University of Colorado, Boulder, CO 3. NASA Langley Research Center, Hampton, VA*



## Abstract

Spectrally resolved up and down-welling actinic flux was measured from aircraft during the Deep Convective Clouds & Chemistry Experiment (DC3) and Tropical Ocean Troposphere Exchange of reactive halogen species and oxygenated VOC (TORERO) campaigns. The measurements were made on the NASA DC-8 and NSF/NCAR G-V with the Charged-coupled device Actinic Flux Spectroradiometer (CAFS) and the HIAPER Airborne Radiation Package (HARP), respectively. Improvements in this instrumentation and the data analysis provide for fast, accurate measurements. Photolysis frequencies calculated from the actinic flux show significant enhancements above clouds. The upwelling signal is enhanced by the high reflectivity of the cloud below. The downwelling is also enhanced due to backscatter of reflected light from the cloud top. Under specific conditions, including high sun and highly reflective clouds, upwelling actinic radiation may exceed the downwelling even with clear skies above. These conditions may have occurred during TORERO and DC3 resulting in regions of highly active photochemistry.


## CAFS/HARP Components

**CCD Monochromator**

- Hamamatsu S7301-906 windowless back-thinned, blue-enhanced, cooled, 534 pix
- Electronics: tec5 timing, cooling, control, acquisition and spectral averaging to minimize detector and read noise
- Housing: Zeiss monolithic ceramic with epoxy attached slit, grating and CCD for temperature and vibration stability
- Wavelength range: 280-680 nm
- Wavelength resolution: ~1.8 nm FWHM at 297 nm
- Accuracy: 5% in UV-B, 3% in UV-A/VIS limited by NIST standards
- Detection limit: ~0.04 mW/m$^2$/nm at 300 nm
- Precision: 1-2% depending on wavelength

**Optical Collector**

**Data Acquisition**

- Small, light, low power PC/104+ computer system
- 16 bit data acquisition
- D/A temperature, pressure and humidity monitoring
- IRIG-B time synchronization
- Custom LabVIEW data acquisition and control software

**Quartz optical collectors**

- 2$\pi$ steradian hemispherical optics
- 30 cm artificial horizon

**Detector and Electronics**

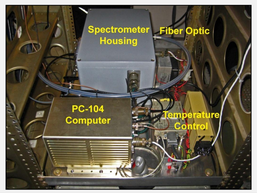


**Fiber Optic Bundles**

- High OH fused silica for high UV throughput

**Detector Specifications**

- Mass: 18 kg / instrument
- Power: 2.5 A of 115 VAC
- Rack Height: 20 cm

## Tropospheric Ultraviolet and Visible Radiation Model

A highly modified TUV version 4+ was used to model the in situ actinic flux for comparison to our measurements. We ran the model using the eight-stream discrete ordinate radiative transfer method with a pseudo-spherical modification. The calculation includes absorption by oxygen and ozone, Rayleigh scattering, and scattering and absorption by aerosols. Standard model conditions consist of cloud free skies, vertical profiles of air, and temperature from the US Standard Atmosphere and Elterman aerosol profile. For comparisons with measured fluxes, total ozone columns from the Ozone Monitoring Instrument (OMI) on the EOS Aura satellite were applied based on the geographical position of the measurement site.

The model was run for every three minutes of measurement using the *in situ* latitude, longitude, altitude, temperature, and pressure and various albedo inputs. TUV was used to generate modeled actinic fluxes with with 1-nm wavelength grid from 292-680 nm. Photolysis frequencies were then calculated from the actinic flux:

$$\text{Photolysis Frequency} = \int F(\lambda)\,\sigma(\lambda,T,p)\,\phi(\lambda,T,p)\,d\lambda$$

The CAFS/HARP and TUV spectra were processed using the same j-value calculation code to ensure that the same quantum yield ($\Phi$), absorption cross section ($\sigma$), temperature ($T$) and pressure (p) dependence relationships were applied to both the measured and modeled spectra.

## Photolysis Frequencies

$j$ [$O_3 \rightarrow O_2+O(^1D)$]

$j$ [$NO_2 \rightarrow NO+O(^3P)$]

$j$ [$H_2O_2 \rightarrow 2OH$]

$j$ [$HNO_2 \rightarrow OH+NO$]

$j$ [$HNO_3 \rightarrow OH+NO_2$]

$j$ [$CH_2O \rightarrow H+HCO$]

$j$ [$CH_2O \rightarrow H_2+CO$]

$j$ [$CH_3CHO \rightarrow CH_3+HCO$]

$j$ [$CH_3CHO \rightarrow CH_4+CO$]

$j$ [$C_2H_5CHO \rightarrow C_2H_5+HCO$]

$j$ [CHOCHO → products]

$j$ [$CHOCHO \rightarrow HCO+HCO$]

$j$ [CH3COCHO → products]

$j$ [$CH_3COCH_3 \rightarrow CH_3CO+CH_3$]

$j$ [$CH_3OOH \rightarrow CH_3O+OH$]

$j$ [$CH_3ONO_2 \rightarrow CH_3O+NO_2$]

$j$ [PAN → products]

$j$ [$CH_3COCH_2CH_3 \rightarrow$ Products]

$j$ [$CH_3CH_2CH_2CHO \rightarrow C_3H_7+HCO$]

$j$ [$CH_3CH_2CH_2CHO \rightarrow C_2H_4+CH_2CHOH$]

$j$ [$HO_2NO_2 \rightarrow HO_2+NO_2$]

$j$ [$HO_2NO_2 \rightarrow OH+NO_3$]

$j$ [$CH_3CH_2ONO_2 \rightarrow$ Products]

$j$ [$Br_2 \rightarrow Br+Br$]

$j$ [$BrO \rightarrow Br+O$]

$j$ [$Br_2O \rightarrow$ products]

$j$ [$BrNO_3 \rightarrow Br+NO_3$]

$j$ [$BrNO_3 \rightarrow BrO+NO_2$]

$j$ [$BrCl \rightarrow Br+Cl$]

$j$ [$HOBr \rightarrow HO+Br$]

$j$ [$BrONO_2 \rightarrow Br+NO_3$]

$j$ [$BrONO_2 \rightarrow BrO+NO_2$]

$j$ [$Cl_2+hv \rightarrow Cl+Cl$]

$j$ [$ClO \rightarrow Cl+O$]

$j$ [$ClONO_2 \rightarrow Cl+NO_3$]

$j$ [$ClONO_2 \rightarrow ClO+NO_2$]

## Convective Impact on Photolysis

ALL DATA IS PRELIMINARY

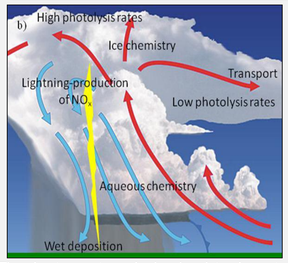


Thunderstorm atmospheric chemistry impacts (Courtesy of NOAA National Weather Service).

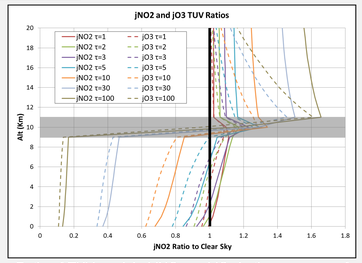


Ratio of TUV modeled $jNO_2$ and $jO_3$ in the presence of a cloud (of varying optical depth) to clear sky. The impact increases with optical depth and the impact on $jO_3$ decreases more rapidly with altitude than for $jNO_2$.

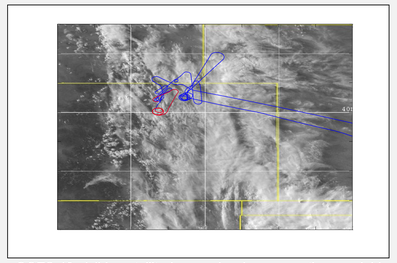

GOES-13 visible satellite image showing convection overlaid with the blue DC-8 flight track (with the spiral and high altitude loop shown at right are highlighted in red).

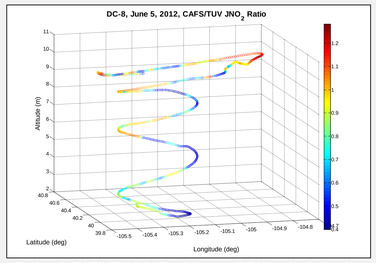


Ratio of CAFS/TUV $jNO_2$ during a DC-8 spiral showing enhanced photolysis above a highly reflective convective cell and strong reduction below the cloud base.

## DC3 Stacked Flight

ALL DATA IS PRELIMINARY

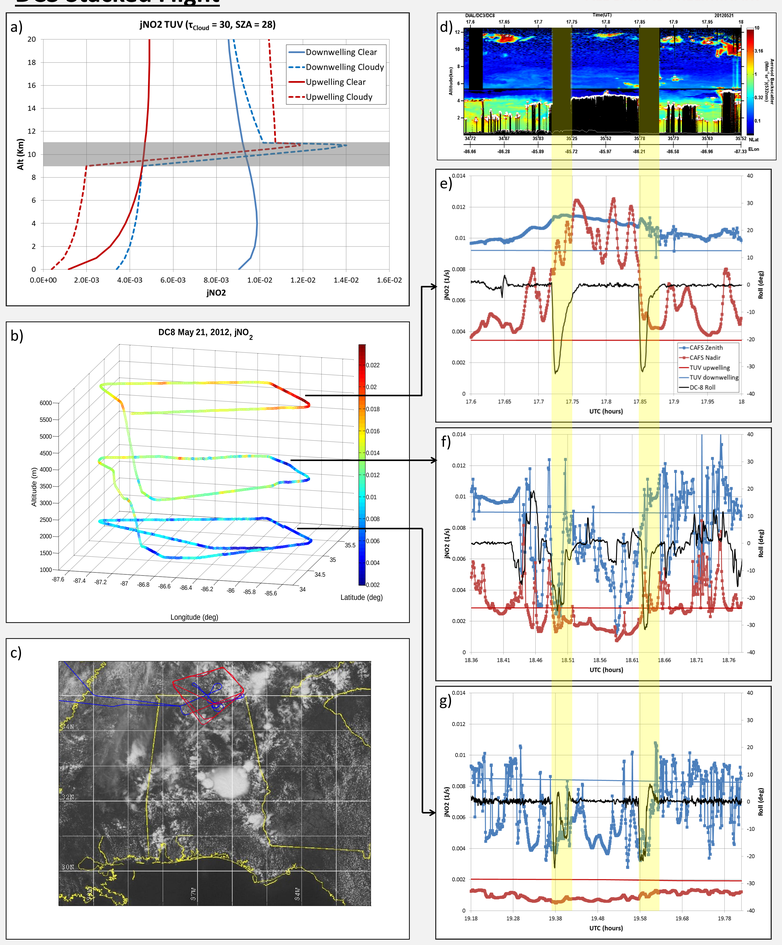


a) TUV modeled up and downwelling $jNO_2$ in the presence of an infinite horizontal cloud at high solar zenith angle. Note upwelling > downwelling photolysis above the cloud.

b) CAFS measured $jNO_2$ along the DC-8 stacked flight legs. The cloud is located along the eastern edge of the stacked boxes and is intersected by the aircraft during middle altitude leg.

c) GOES-13 visible satellite image showing convection intersected by the DC-8 track (stacked flight legs in red).

d) DIAL 532 nm aerosol backscatter indicating cloud locations along the horizontal flight track (near 5.5 km).

e,f,g) CAFS and clear-sky TUV $jNO_2$ along the flight track for each stacked leg. Aircraft turns (yellow bars) are nearly coincident with the cloud edge. Note in (e) CAFS nadir > zenith (upwelling > downwelling) above the cloud.

## TORERO Cloud Overpass

ALL DATA IS PRELIMINARY

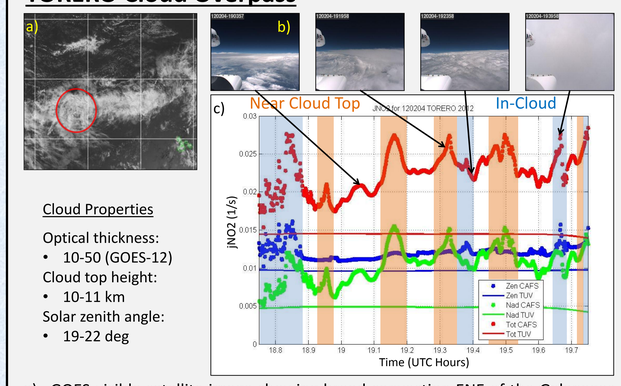


Cloud Properties

Optical thickness:
- 10-50 (GOES-12)

Cloud top height:
- 10-11 km

Solar zenith angle:
- 19-22 deg

a) GOES visible satellite image showing broad convection ENE of the Galapagos islands intercepted by the G-V in the red circle region

b) Images from the G-V forward camera on the starboard wing showing the variability in the cloud structure. The final image shows the aircraft flying through convective blow off above the cloud base.

c) CAFS and clear-sky TUV $jNO_2$ along the flight track. The upwelling is enhanced by the high reflectivity of the cloud below. The downwelling is also enhanced due to backscatter of reflected light from the cloud top. The effect is stronger near the cloud tops and strongest within and near the top of the cloud.

## Further analysis

The DC3 and TORERO studies provide a rich database for study of atmospheric photolysis frequencies in the presence of convection and optically thick clouds. The strong reflectivity results in regimes of both highly enhanced and suppressed photochemistry under complex dynamical conditions. Further study will include

- Case study analysis of photolysis rates in the vicinity of convective towers and anvil penetrations.
- Statistical analyses of the regimes above, within and below optically thick clouds. New research by Palancar et al., (2011) demonstrates that up and downwelling actinic flux measurements exhibit distinct modal behavior dependent on cloud and aerosol morphology when compared with a clear sky model.
- Collaborative studies to assess the impact of the photochemical environment on convectively redistributed species and the impacts on the UT/LS, cirrus and cumulus anvil regimes, biomass burning plumes and local air quality.
- Collaborative studies to assess the radiative environment across the full spectrum including calculation of the layer absorption coefficient, *in situ* effects of aerosol variability on actinic flux and feedbacks to the chemistry and aerosol evolution.


**Acknowledgements**: NCAR is operated by the University Corporation for Atmospheric Research under the sponsorship of the National Science Foundation (NSF). This DC3 research is funded by NASA under award No. NNX12AB82G S01 and NSF. The TORERO project is funded by the NSF under award AGS-1104104 (PI: Volkamer). The involvement of the NSF-sponsored Lower Atmospheric Observing Facilities, managed and operated by NCAR Earth Observing Laboratory, is acknowledged. Special thanks to all collaborators and logistic team members.